RSC Advances

PAPER

View Article Online
View Journal | View Issue

Cite this: *RSC Adv.*, 2018, **8**, 38118

Analysis of effect of oil and S^{2-} impurities on corrosion behavior of 16Mn steel for storage tanks by electrochemical method

Zhao Xiaodong, *[a] Chen Kefeng,[bc] Yang Jie,[a] Xi Guangfeng,[d] Sun Jie[a] and Tian Haitao[a]

Received 30th September 2018
Accepted 2nd November 2018

DOI: 10.1039/c8ra08113a

rsc.li/rsc-advances

Corrosion is a common problem of storage tanks, and different storage media and impurities have different effects on the corrosion behavior of steel used for tanks. In this paper, electrochemical impedance spectroscopy (EIS) and polarization curves were used to study the corrosion behavior of 16Mn steel in 3.5% sodium chloride solution after immersion in heavy oil, diesel oil and gasoline, considering the influence of the main impurities, S^{2-}, on the corrosion process. The results showed that the self-corrosion current density of 16Mn steel in the solution after the immersion in gasoline was higher than that in heavy oil and diesel oil, due to the higher dissolved oxygen concentration promoting the cathodic reaction. The comparison of blank sample in 3.5% sodium chloride solution and the immersed samples showed that the corrosion rate of the 16Mn steel decreased in the presence of an oil film on the surface of the steel. With the increase of S^{2-} concentration in the oil, the corrosion rate of 16Mn steel tended to be stable after it gradually increased. This was mainly related to the composition of FeS and FeS_{1-x} in the sulfide film formed on the surface of the steel as well as the change of the lattice structure.

Introduction

With the development of the oil industry and oil transportation, there are increasingly high requirements for storage tanks. However, corrosion is a common problem of oil storage tanks. The damage caused by corrosion has greatly affected the service life of tanks and also increased its insecurity.[1] There are two main reasons for corrosion of storage tanks:[2–4] first, the corrosion is caused by external environmental factors. The other is that the oil stored in the tank also has an influence on the inner wall of the storage tank. According to the nature of oil stored, the steel tanks can be divided into heavy oil tanks and light oil tanks. Light oil usually refers to the storage medium as a solvent oil, diesel, gasoline, naphtha, kerosene and other light oil products, while heavy oil tanks are used for storage of high viscosity, high condensation point oil, usually the residual heavy oil after extraction of the gasoline and diesel from the crude oil with high molecular weight and high viscosity. Oil corrosion of the metal is caused by non-hydrocarbon impurities such as the active sulfide, water-soluble acid or alkali. The active sulfide refers to the petroleum or petroleum products that can directly interact with the equipment metal and lead to its corrosion, including mercaptans, thiophenol, elemental sulfur and hydrogen sulfide.

At present, a lot of research has been done on the corrosion factors and corrosion process of oil storage tanks. Foroulis[5] discussed the effect of hydrogen sulfide content in tanks on the corrosion of carbon steel. Zhang *et al.*[6] analyzed the relationship between the properties of crude oil and the corrosion behavior of 16Mn steel in storage tanks by the gray relational method, showing the main reason for the corrosion of crude oil storage tanks was salinity, then followed by sulfur content. Kong *et al.*[7] analyzed the corrosion of Q235 steel caused by residual oil, indicating that the residual oil had a relationship with steel corrosion rate under static and flowing conditions. Efird *et al.*[8] investigated the corrosive effect of crude oil in crude oil/brine on steel, showing that the addition of crude oil to brine reduced the corrosion rate of steel. The EIS is a method widely used for monitoring the metal corrosion and for the evaluation of heterogeneous charge-transfer parameters and for studies of double layer structure.[9,10] And the Nyquist and Bode graphs obtained from EIS can better reflect the corrosion mechanisms, especially the cathodic corrosion controlled by the dissolved oxygen. In order to systematically study the effect of different oil and impurity on the corrosion behavior of 16Mn steel used for storage tank, three kinds of oil products, including heavy oil, diesel oil and gasoline, were selected as the representative, and

[a]School of Ocean, Yantai University, Yantai 264005, China. E-mail: danielxdzhao@aliyun.com
[b]School of Naval Architecture and Mechanical-electrical Engineering, Zhejiang Ocean University, Zhoushan 316022, China
[c]Key Laboratory of Marine Materials and Related Technologies, Ningbo Institute of Materials Technology and Engineering, Chinese Academy of Sciences, China
[d]Shandong Special Equipment Inspection Institute Lute Inspection & Testing Co. Ltd, Jinan 250100, China

Na_2S was used to provide different concentrations of S^{2-} to simulate sulfide impurities in oil products. Then the corrosion behavior of the steel was studied by electrochemical impedance spectroscopy and polarization curves.

Experimental

Materials

The steel samples used in this experiment as working electrodes were cut from a 16Mn steel plate, and the composition was as follows (wt%): C 0.13–0.18, Si 0.20–0.60, Mn 1.20–1.60, P ≤ 0.030, S ≤ 0.030, Ni ≤ 0.30, Cr ≤ 0.30, Cu ≤ 0.25. Then the samples were sealed with epoxy resin leaving a square working area of 1 cm^2 exposed to the electrolyte, and the non-working surface was weld with copper wire. Before the experiment, the working surfaces were abraded with a series of silicon carbide papers (up to 1500), and then washed with distilled water and degreased in acetone and dried. After immersion in heavy oil, diesel and gasoline for 15 days, respectively, the steel samples were placed in 3.5% sodium chloride solution for electrochemical measurements, with blank samples directly immersed in 3.5% sodium chloride solution for comparison. In addition, $Na_2S{\cdot}9H_2O$ was used for the preparation of 3.5% sodium chloride solution with 0.5%, 1.5%, 2.5% and 3.5% S^{2-} concentrations.

Electrochemical measurements

A Princeton 2273 electrochemical workstation was used to conduct electrochemical tests using a classical three-electrode system. The reference electrode was a saturated calomel electrode (SCE) and the auxiliary electrode was a platinum electrode. Electrochemical impedance spectroscopy was performed in the frequency range of 10 MHz to100 KHz and the amplitude of the sinusoidal voltage signal was 10 mV. The polarization curve was tested in a scanning range of −350 mV to +350 mV at a scanning rate of 0.333 mV s^{-1}.

Results

Electrochemical behavior of 16Mn steel after immersion in different oil

Fig. 1 and 2 show the Nyquist and Bode diagrams of the 16Mn steel (including blank samples) in 3.5% NaCl solution after immersed in heavy oil, diesel and gasoline for 15 days, respectively. In all the curves, there were two capacitive reactance arcs in the Nyquist diagrams and two time constants in the Bode diagrams. The high frequency capacitive reactance arc corresponded to the capacitance of the oil film and the micropore resistance on the surface of the oil film, and the reactance arcs in medium and low frequency area were related to the double layer capacitance on metal matrix interface and charge transfer resistance of metal reaction.[11,12] From the Nyquist diagram, it showed that the radius of capacitive arc of the sample immersed in heavy oil was the largest, then followed by diesel oil and gasoline, while the sample immersed directly in NaCl solution had the smallest capacitance radius, indicating that 16Mn steel

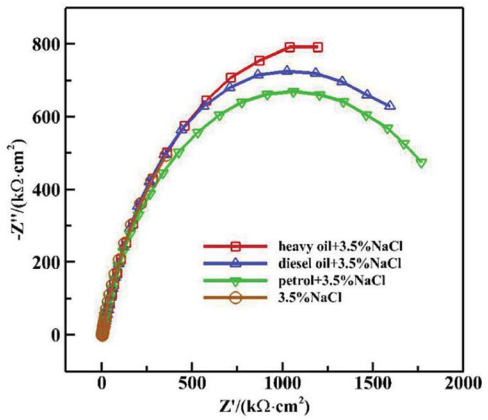

Fig. 1 Nyquist diagram of 16Mn steel in 3.5% NaCl solution after immersed in different oil for 15 days.

immersed in heavy oil had the least corrosion tendency, then followed by diesel, gasoline and the blank sample. During the samples taken out from the oil and immersed in sodium chloride solution, the amount of the oil film of the most volatile gasoline attached to the surface of the steel was the least. The chloride ions were easy to be adsorbed on the surface of metal and react with the metal substrate for their small radius and penetration ability.[13,14] At the same time, the high dissolved oxygen concentration in gasoline[15] promoted the cathodic oxygen absorption reaction and accelerated the corrosion rate of 16Mn steel. In addition, the Nyquist diagram showed that the 16Mn steel immersed in oil had a relatively large modulus compared to the 16Mn steel directly immersed in 3.5% NaCl. The Bode diagrams revealed that the impedance spectra in three different oils overlapped in the high frequency area, indicating that the experiment was in the middle stage of immersion and the permeation of the ions through the oil film reached a saturation state.[16]

In order to study the electrochemical corrosion behavior of 16Mn steel quantitatively, the EIS are fitted with the equivalent circuit (Fig. 3). The fitting parameters obtained are shown in

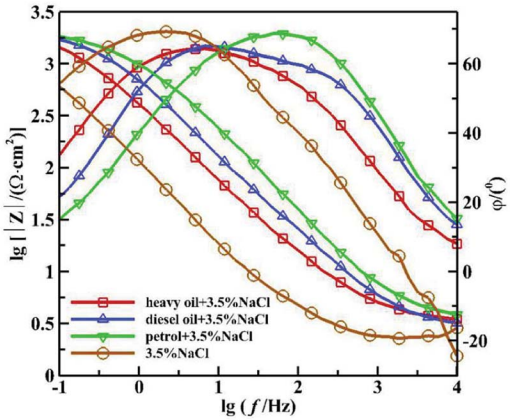

Fig. 2 Bode diagram of 16Mn steel in 3.5% NaCl solution after immersed in different oil for 15 days.

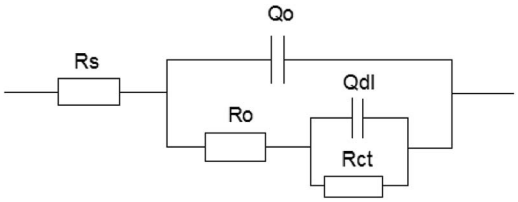

Fig. 3 The equivalent circuit model used to fit the EIS experimental data for 16Mn steel in 3.5% NaCl solution after immersed in different oil for 15 days.

Table 1. In the equivalent circuit model, R_s represents an electrolyte resistance, R_o and Q_o represent a resistance and a capacitance of the oil film, R_{ct} and Q_{dl} represent a charge transfer resistance and a double layer capacitance, respectively. The fitting results showed that the total resistance of the 16Mn steel immersed in heavy oil was the highest in the solution, indicating that the corrosion resistance of the 16Mn steel immersed in the heavy oil was the highest. Since the heavy oil film was not easy to fall off, corrosive medium was not easy to penetrate and the corrosion of the metal substrate was less affected. The charge transfer resistance of the 16Mn steel immersed in the three oils was consistent with the results reflected in the Nyquist diagrams of the capacitive arc radius.

Fig. 4 shows the polarization curves of 16Mn in sodium chloride solution after immersion in different oils. Table 2 shows the electrochemical parameters obtained after fitting the polarization curves in the Tafel zone using C-view software. As shown from the diagram, the slope of the anodic polarization curves did not change much in the Tafel zone, while the slope of the cathodic polarization curves was significantly larger than that of the anodic polarization curves, indicating that the reaction resistance was large and the corrosion was controlled by the cathodic process. As mentioned above, the oil film attached to the steel surface inhibited the cathode reaction.

From the fitting data in Table 2, it is seen that the self-corrosion potentials of 16Mn steel obtained in sodium chloride solution after immersion in heavy oil, diesel oil and gasoline were 1.18×10^{-6} A cm^{-2}, 1.25×10^{-6}A cm^{-2} and 3.15×10^{-6}A cm^{-2}, respectively, indicating that the corrosion rate of 16Mn steel immersed in gasoline was larger than that in other two kinds of oil products, but all the corrosion current densities were not very large.

In addition, the polarization curves showed that the corrosion potential of 16Mn steel directly immersed in 3.5% NaCl solution showed a significant negative shift, which also showed that the oil attached to the surface of 16Mn steel had a corrosion inhibition effect.[17] The inhibition material adsorbed on the surface of the metal produced a dense film and inhibited the corrosion reaction in the active region of the sample surface, hindered the transfer of the corrosive medium and the corrosion product and reduced the corrosion rate of the 16Mn steel.

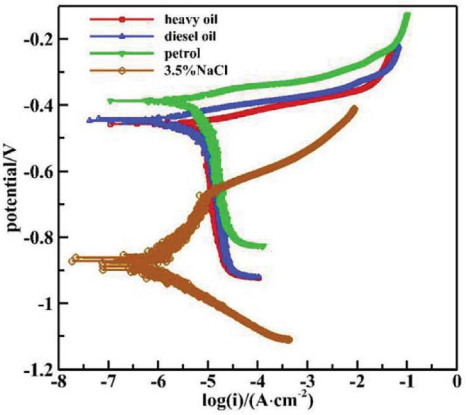

Fig. 4 Polarization curves of 16Mn steel in sodium chloride solution after immersed in different oils.

Hazlewood *et al.*[18,19] pointed out the factor that caused the corrosion damage to the crude oil storage tank was not the crude oil itself. In fact, the crude oil was not corrosive to the metal materials in contact with the oil tank. Moreover, the oil film even had corrosion inhibition to the inner layer of the steel. While in the other parts of the tank, such as the top of the tank, the outer layer without the protection of the oil film was easily subject to the corrosive media.

Electrochemical behavior of 16Mn steel in NaCl solution with different S^{2-} concentrations

Fig. 5 shows the Nyquist diagrams of AC impedances of 16Mn steel in NaCl solution with different S^{2-} concentrations. As is seen from Fig. 5, the impedance spectroscopy varied obviously with different S^{2-} concentrations. The arc radius of capacitive reactance changed much and the corrosion tendency of 16Mn steel increased with the S^{2-} concentration and then tended to be stable. At small concentration of sulfur ions, the corrosion product film had a protective effect. While with the increase of the concentration of sulfide ions, the composition and structure of the product film had changed, the protective effect decreased, the corrosion rate increased and then tended to be stable.

The following equivalent circuit (see Fig. 6) is obtained using the Zsimpwin software and the fitting parameters are shown in Table 3. In the equivalent circuit model, R_s represents an electrolyte resistance, R_{ct} and Q_{dl} represent a charge transfer resistance and a double layer capacitance respectively, and R_w

Table 1 Fitting parameters derived from equivalent circuit model in Fig. 3

Medium	R_s (Ω cm^2)	$Q_o \times 10^{-4}$ (Ω^{-1} cm^{-2})	n_1	R_o (kΩ cm^2)	$Q_{dl} \times 10^{-4}$ (Ω^{-1} cm^{-2})	n_2	R_{ct} (kΩ cm^2)
Heavy oil + 3.5% NaCl	3.312	5.145	0.75	84.84	0.5437	0.85	2263
Diesel oil + 3.5% NaCl	2.249	3.569	0.77	232	0.2438	0.8	1413
Petrol + 3.5% NaCl	2.816	1.71	0.82	1069	9.628	0.62	701.3
3.5% NaCl	1.943	4.677	0.85	4.439	20.66	0.77	1387

Table 2 Electrochemical parameters of Tafel polarization curves in Fig. 4

Medium	I $\times 10^{-6}$ (A cm^{-2})	E sec (V)
Heavy oil + 3.5% NaCl	1.18	−0.479
Diesel oil + 3.5% NaCl	1.25	−0.443
Petrol + 3.5% NaCl	3.15	−0.389
3.5% NaCl	1.22	−0.886

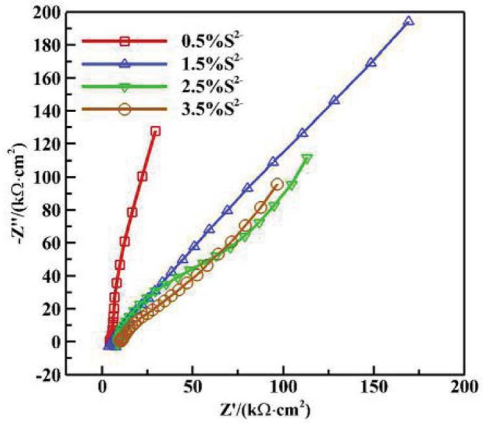

Fig. 5 Nyquist diagrams of AC impedances of 16Mn steel in NaCl solution with different S^{2-} concentrations.

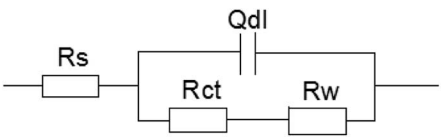

Fig. 6 The equivalent circuit model used to fit the EIS experimental data for 16Mn steel in NaCl solution with different S^{2-} concentrations.

represents a diffusion resistance. The fitting data showed that R_{ct} reached its minimum value at the sulfur ion concentration of 3.5%, indicating that the corrosion tendency was the highest at this concentration and increased rapidly in the initial stage and then tended to be gentle. In addition, R_{ct} value at the sulfur ion concentration of 2.5% was equivalent with that at the concentration of 2.5%, indicating that the corrosion rate tended to be stable when the sulfur ion concentration was large enough.

Fig. 7 shows the polarization curves of 16Mn steel in NaCl solutions with different S^{2-} concentrations and the fitting result is summarized in Table 4. It is seen from the polarization curves that as the S^{2-} concentration increased, the self corrosion potential of 16Mn steel shifted negatively, indicating that the corrosion tendency of 16Mn steel increased to a certain extent with the sulfur ion concentration. In addition, the slope of the anodic polarization curve was obviously larger than that of the cathodic polarization curve, revealing that the corrosion reaction was controlled by the anodic process. The self corrosion current density fitted in the Tafel zone increased with the sulfide ion concentration, from 2.2464 μA cm^{-2} to 8.5439 μA cm^{-2}. It was consistent with the results obtained by the AC impedance spectroscopy.

Discussions

From the results of EIS and polarization curves, compared with the blank sample, the corrosion resistance of the 16Mn steel after immersion in the oil was improved, indicating that the oil film had a protective effect. The experimental data of the three oils were in the same order of magnitude, showing that the influence of all oils on the material was similar. The three oils were a class of mixture containing alkanes, cycloalkanes, aromatic hydrocarbons and other substances, and contained a large number of hydrophobic group C–H bonds.[20,21]

The sample surface has a certain roughness, according to Young equation:[22]

$$\cos\theta = \frac{\gamma_{g-s} - \gamma_{l-s}}{\gamma_{g-l}} \quad (1)$$

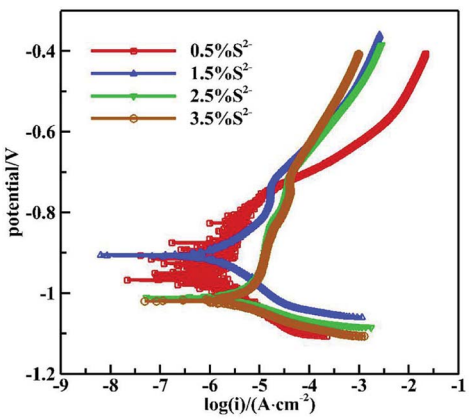

Fig. 7 The polarization curves of 16Mn steel immersed in different S^{2-}concentration solutions.

Table 3 Fitting parameters derived from equivalent circuit model in Fig. 6

[S^{2-}] (wt%)	R_s (Ω cm^2)	Q $\times 10^{-3}$ (Ω^{-1} cm^{-2})	n	R_{ct} (kΩ cm^2)	$R_w \times 10^{-3}$ (Ω cm^2)
0.5	3.49	2.94	0.761	966	5.67
1.5	22.38	4.32	0.758	99.12	4.32
2.5	15.77	6.19	0.757	34.12	9.82
3.5	50.96	30.3	0.759	29.33	10.03

Table 4 Electrochemical parameters of Tafel polarization curves in Fig. 7

$[S^{2-}]$ (wt%)	I $\times 10^{-6}$ (A cm^{-2})	E sec (V)
0.5	2.2464	−0.7586
1.5	2.7009	−0.7231
2.5	8.4576	−0.8105
3.5	8.5439	−0.8199

θ is contact angle, γ_{g-s} is gas–solid interface free energy, γ_{l-s} is liquid–solid interface free energy, and γ_{g-l} is gas–liquid interface free energy.

After immersion in the oil, due to different contact angle, the adhesion ability varied with different surface. The oil film covering the surface was inhomogeneous, and there was even small area of the surface leaving uncovered ($\theta > 90°$). Therefore, when the samples with the oil film immersed in 3.5% NaCl solution were tested, the oil-protected areas might have better corrosion resistance, while the exposed surface of the sample was prone to local corrosion or "pitting".

In addition, there was a difference in dissolved oxygen content among the three kinds of oils. Generally, under the same conditions, the liquid with good liquidity maintained good contact with the air. Because of the relatively small molecular weight and certain volatility of gasoline among the three liquids, it had the best liquidity and the dissolved oxygen concentration was also relatively higher. The polarization curves in Fig. 4 showed that the corrosion reaction was controlled by the cathode reaction caused by the diffusion of oxygen concentration in the experiments. The larger the dissolved oxygen content, the easier it was to promote the cathode reaction. The self corrosion current density in the fitting parameters also reached its maximum value.

Impurities cannot be avoided in the oil product, among which sulfur ions is an important factor affecting the material corrosion. As the concentration of sulfur ions increased, the surface of the sample was covered with a layer of corrosion product, and its compactness also varied with the sulfur ion concentration.[23]

The corrosion product film is mainly composed of sulfides. The corrosion mechanism of sulfur ions on 16Mn steel can be described as the following chemical equations.

Sulfur ions penetrate the layer and react with Fe^{2+}:

$$S^{2-} + Fe^{2+} \rightarrow FeS \quad (2)$$

Sulfur ions are reduced to HS^-:

$$S^{2-} + H_2O \rightarrow HS^- + OH^- \quad (3)$$

The resulting HS^- with a strong adsorption capacity adsorbed on the sample surface:

$$HS^- + Fe \rightarrow Fe\,(HS^-)_{ads} \quad (4)$$

Anode reaction:

$$Fe(HS^-)_{ads} \rightarrow Fe(HS^+)_{ads} + 2e \quad (5)$$

Finally,

$$Fe(HS^+) \rightarrow FeS_{1-x} + xHS^- + (1 - x)H^+ \quad (6)$$

$$Fe(HS^+)_{ads} + HS^- \rightarrow FeS + H_2S \quad (7)$$

According to the above equations, a corrosion product layer was gradually formed on the surface of the sample, and the main sulfides were FeS and FeS_{1-x}. FeS generated in the early stage had a certain protective effect. According to Le Chatelier's principle,[24] increase of the concentration of sulfide ions promoted the reaction to move in the forward direction. With the increase of S^{2-} content, the corrosion products transformed into $Fe_{1-x}S$ with large difference between crystal lattice and the steel substrate, which was loose and easy to fall off, leading to the acceleration of corrosion.

Conclusions

The corrosion current densities of 16Mn steels in 3.5% NaCl solution after immersion in heavy oil, diesel oil and gasoline for 15 days tested in the electrochemical experiments were 1.18×10^{-6} A cm^{-2}, 1.25×10^{-6} A cm^{-2} and 3.15×10^{-6} A cm^{-2}, respectively. It showed that the corrosion tendency of 16Mn steel after immersion in petrol oil film was the largest, which was mainly related to the concentration of dissolved oxygen contained in the oil products. As a blank sample without immersion in oil, the corrosion potential in 3.5% NaCl solution was more negative than those in the oils, indicating that the attachment of the oil film inhibited the corrosion to a certain extent.

The electrochemical behavior of 16Mn steel in NaCl solution with different S^{2-} concentrations showed that the corrosion current density of 16Mn steel increased with S^{2-} concentration and then stabilized, which was related to the formation and transformation of sulfide film, mainly composed of FeS and FeS_{1-x}, as well as changes in the lattice structure of the corrosion product layer.

Conflicts of interest

There are no conflicts to declare.

Acknowledgements

This research was supported by Foundation of Key Laboratory of Marine Materials and Related Technologies, Ningbo Institute of Materials Technology and Engineering, Chinese Academy of Sciences (Grant No. 2017Z01). The support from Scientific Research Foundation of Yantai University (Grant No. HX17B38) is also gratefully acknowledged.

Notes and references

1 X. Hao and J. Dong, *Corros. Sci.*, 2016, **110**, 296.

2 A. R. Ramírez, J. S. D. Mason and N. Pearson, *NDT&E Int.*, 2009, **42**, 16.
3 F. H. Meyer, O. L. Riggs and R. L. McGlasson, *Corrosion*, 1958, **14**, 69.
4 S. Wang, *Corros. Prot. Petrochem. Ind.*, 2011, **4**, 12.
5 Z. A. Foroulis, *Anti-Corros. Methods Mater.*, 1981, **28**, 4.
6 Z. Yanfei, C. Xu and H. E. Chuan, *J. Chin. Soc. Corros. Prot.*, 2015, **35**, 43.
7 X. Kong, J. Han and D. Chen, *Science Technology and Engineering*, 2010, **29**, 37.
8 K. D. Efird and R. J. Jasinski, *Corrosion*, 1989, **45**, 165.
9 R. Martin, Dynamic optimization of chemical additives in a water treatment system, *US Pat* 6419817, 2000.
10 K. Fei, Z. Jinna and Z. Changjun, *Recent Pat. Corros. Sci.*, 2010, **2**, 34.
11 X. Zhao, S. Liu and X. T. Wang, *Chin. J. Oceanol. Limnol.*, 2014, **32**, 1163.
12 S. Liu, H. Y. Sun and L. J. Sun, *Corros. Sci.*, 2012, **65**, 520.
13 S. J. Stuart and B. J. Berne, *J. Phys. Chem. A*, 1999, **103**, 10300.
14 I. B. Beech and J. Sunner, *Curr. Opin. Biotechnol.*, 2004, **15**, 181.
15 Z. J. Wang, B. F. Qi and B. Gao, *Guangdong Chem. Ind.*, 2011, **38**, 145.
16 C. N. Cao and J. Q. Zhang, *An Introduction to Electrochemical Impedance Spectroscopy*, 2002, vol. 158.
17 G. H. Booth and A. K. Tiller, *Corros. Sci.*, 1968, **8**, 583.
18 P. E. Hazlewood, *Factors affecting the corrosivity of pulping liquors*, Georgia Institute of Technology, 2006.
19 D. C. Crowe and R. A. Yeske, *Kraft White Liquor Composition and Long Term Corrosion Behavior*, NACE, 1988, p. 435.
20 D. M. Padlo, *Fuel Process. Technol.*, 1996, **49**, 247.
21 G. B. Adebayo and O. M. Ameen, *J. Microbiol. Biotechnol. Res.*, 2017, **1**, 12.
22 A. W. Adamson and A. P. Gast, *Physical chemistry of surfaces*, A Wiley-Interscience Publication, 6th edn, 1997.
23 D. D. MacDonald, B. Roberts and J. B. Hyne, *Corros. Sci.*, 1978, **18**, 411.
24 H. D. B. Jenkins, *Chemical thermodynamics at a glance*, 2008, p. 160.